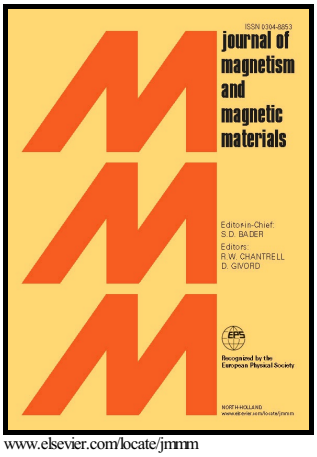

www.elsevier.com/locate/jmmm

Exchange-spring driven spin-flop transition in $DyFe_2/YFe_2$ superlattices

D. Wang, A.R. Buckingham, G.J. Bowden, R.C.C. Ward, P.A.J. de Groot

PII: S0304-8853(15)30647-8
DOI: http://dx.doi.org/10.1016/j.jmmm.2015.10.015
Reference: MAGMA60708

To appear in: *Journal of Magnetism and Magnetic Materials*

Received date: 6 March 2014
Revised date: 28 September 2015
Accepted date: 8 October 2015

Cite this article as: D. Wang, A.R. Buckingham, G.J. Bowden, R.C.C. Ward and P.A.J. de Groot, Exchange-spring driven spin-flop transition in $DyFe_2/YFe$ superlattices, *Journal of Magnetism and Magnetic Materials* http://dx.doi.org/10.1016/j.jmmm.2015.10.015

Exchange-spring driven spin-flop transition in $DyFe_2/YFe_2$ superlattices

D. Wang[a], A. R. Buckingham[b], G. J. Bowden[b], R. C. C. Ward[c], P. A. J. de Groot[b,1]

[a] *School of Physics and Electronics, Central South University, Changsha 410083, China*
[b] *School of Physics and Astronomy, University of Southampton, Southampton SO17 1BJ, UK*
[c] *Clarendon Laboratory, Oxford University, Oxford OX1 3PU, UK*

Abstract

Exchange-spring driven spin-flop transition is observed in hysteresis loops of an antiferromagnetic [$DyFe_2$ 40Å/YFe_2 160Å] × 20 superlattice at temperatures higher than 100 K, with field along the in-plane easy axis [$\bar{1}10$]. OOMMF micromagnetic simulation reveals that this transition is derived from the magnetoelastic interaction in $DyFe_2$. Conventional exchange spring behavior is also observable at smaller fields. Simulation shows that it is caused by the simultaneous rotation of the magnetization vectors of both the hard and soft layers towards [010]. Experiment and simulation agree qualitatively with each other.

Keywords: $DyFe_2/YFe_2$ superlattices, Exchange spring, Spin-flop transition

1. Introduction

Exchange spring systems [1] recently have attracted a great deal of interest, as they offer promising solutions to maximizing the energy product [2], $(BH)_{max}$, of a permanent magnet and overcoming the superparamagnetic limit for a small magnetic particle used as an information element [3]. The current research on exchange spring magnets can be divided into two categories: ferromagnetic (FM) and antiferromagnetic (AFM). For the FM coupled exchange systems, the main objective is to increase the energy product. A SmCo/Fe system is a good example of this and many excellent results have been obtained [4]. On the AFM side, single crystal $DyFe_2/YFe_2$ superlattices are studied extensively [5] as a model system to investigate the miscellaneous facets of exchange-spring related phenomena. Recent advances [6] on this system lend more insight into the exchange-spring driven magnetization reversal processes in AFM coupled superlattices.

Email address: dwwang@nudt.edu.cn (D. Wang)
[1] Deceased

X-ray magnetic circular dichroism (XMCD) study of a soft-dominant (110) [$DyFe_2$ (50 Å)/YFe_2 (200 Å)] × 13 superlattice sample demonstrated that there was a transition of switching mode when the temperature was increased [7]. At low temperature, the Dy hysteresis was square, resembling the easy-axis response of a hard magnet with uniaxial anisotropy, while the Y edge signal gave an almost square hysteresis loop with a reduced coercivity. However, the high temperature element specific XMCD signals were very complicated, especially for the Dy edge signal [7]. This switching mode transition was later explained by an energy argument in a micromagnetic simulation [8]. The experiment and simulation agreed qualitatively with each other. However, the important magneto-elastic contribution to the anisotropy of $DyFe_2$ was not fully taken into account in the micromagnetic simulation study. Adding to the complexity, in order to model the neutron scattering data obtained from a (110) [$DyFe_2$ (30 Å)/YFe_2 (120 Å)] × 22 superlattice sample at 250 K, the interface exchange coupling constant had to be reduced in magnitude by one or two orders from those of the constituent layers [10]. In this article, we find that a fully taken into account magneto-elastic contribution can lead to a spin-flop transition [9] of the $DyFe_2$ moments, still in agreement with the XMCD and neutron scattering experiments, while the dramatic reduction in interface exchange is not necessary. This finding highlights the importance of knowing the detailed magnetic interactions in the interpretation of magnetometry data. In passing, we would like to note that a similar spin-flop transition has been observed in antiferromagnetically-coupled $ErFe_2/YFe_2$ superlattices by traditional magnetometry [11] and XMCD measurements [12].

2. Experimental and theoretical details

The sample used is a (110) [$DyFe_2$ 40 Å/YFe_2 160 Å] × 20 superlattice. It is grown by molecular beam epitaxy (MBE), with atomically sharp interfaces [13]. The superlattice is characterized by strong FM exchange coupling between Fe-Fe (∼ 600 K). The exchange between Dy-Fe is AFM, of the order ∼ 100 K. The FM exchange between Dy-Dy is well below 100 K. So the effective exchange coupling between $DyFe_2$ and YFe_2 is AFM. The hysteresis loops were measured using an Oxford Instruments Aerosonic 3001 vibrating sample magnetometer (VSM), with a maximal field of 12 T.

Both the crystal field and magneto-elastic interactions in the soft YFe_2 are negligible. The cubic magneto-crystalline anisotropy of the hard $DyFe_2$ is mainly derived from the crystal field at Dy sites [14]. In its bulk form, the strain and hence the magneto-elastic energy in $DyFe_2$ are negligible, and the easy axes are determined by the magneto-crystalline anisotropy solely, being along with <001> directions, irrespective of the temperature. However, due to the elevated temperature needed for the deposition of the superlattice [13], this is not the case anymore for $DyFe_2$ in the form of an epitaxial film. Due to the different thermal contraction experienced by the superlattice and the substrate during the process of cooling down to room temperature, a shear strain of the order of $\epsilon_{xy} \sim -0.55\%$ (z axis is along [110], the growth direction of the film) will

develop in the superlattice [16]. The other components of the strain are small and make negligible contribution to the magneto-elastic energy. At low temperature, the corresponding magneto-elastic energy is small, as compared to the large magneto-crystalline anisotropy. So the easy axes are still determined by the magneto-crystalline anisotropy. But, due to the rapid temperature variation of the magneto-crystalline anisotropy, at room temperature the magneto-elastic energy becomes the dominant contribution, which results in the observed transition of the in-plane easy axis from $[00\bar{1}]$ to $[\bar{1}10]$ [17]. Theoretical calculations [15] based on the single-ion model confirmed this change in relative importance for the determination of easy axes. To make a better agreement with experiment, especially the $\sim 14^\circ$ out-of-plane angle for $DyFe_2$ at room temperature [18, 19], a factor of 2.5 [20] has to be multiplied to the magneto-elastic anisotropy obtained from the single-ion model. In contrast, the previous micromagnetic study [8] of the same system used the as-derived magneto-elastic anisotropy. The different treatment of the magneto-elastic anisotropy leads to the different switching modes observed.

OOMMF micromagnetic simulation [21] had been used to understand the complicated switching modes in exchange spring systems [8]. Significant insight into the exchange spring formation process can be gained by combining both experiment and simulation. In the current simulation, the whole superlattice is discretized into one dimensional (1D) exchange coupled spins. The discretization length is 1 nm, in consideration of the 3.4 nm exchange length [8]. Due to the 1D character of the simulation, demagnetization effect is not included. The values $A_s = A_h = -A_i = 1.46 \times 10^{-11}$ J/m are used in the simulation, where A_s, A_h and A_i are the exchange coupling constants in the soft layers, in the hard layers and at the hard/soft interfaces, respectively. Other temperature dependent parameters, such as magnetization and the anisotropy constants, are given in Ref. [15]. Simulation details are given in Ref. [8].

3. Results

A typical hysteresis loop, measured at 250 K with the applied field along $[\bar{1}10]$, can be seen in Fig. 1. The small field (-0.35 T $< B_{app} < 0.35$ T) feature is reminiscent of the exchange spring winding in the soft phase, and the abrupt switching at approximately -0.3 T resembles the simultaneous 180° rotation of both the hard and the soft phases, as observed in a similar superlattice at room temperature using magneto optic Kerr effect [22]. The whole demagnetization process can be obtained from OOMMF simulation. As noted before [8], in order to accommodate finite temperature effects, a higher temperature value has to be used. Here a temperature of 380 K is adopted. The simulated hysteresis loop, together with the element specific loops for $DyFe_2$ and YFe_2, can be seen in Fig. 2. The qualitative agreement to the experimental curve is obvious. Quantitatively, due to the Brown's paradox [23], the simulated zero-temperature characteristic fields are significantly larger than the experimental ones.

The demagnetization process as obtained from the OOMMF simulation is as follows: At 20 T, the system is in a perpendicular state, with the soft mag-

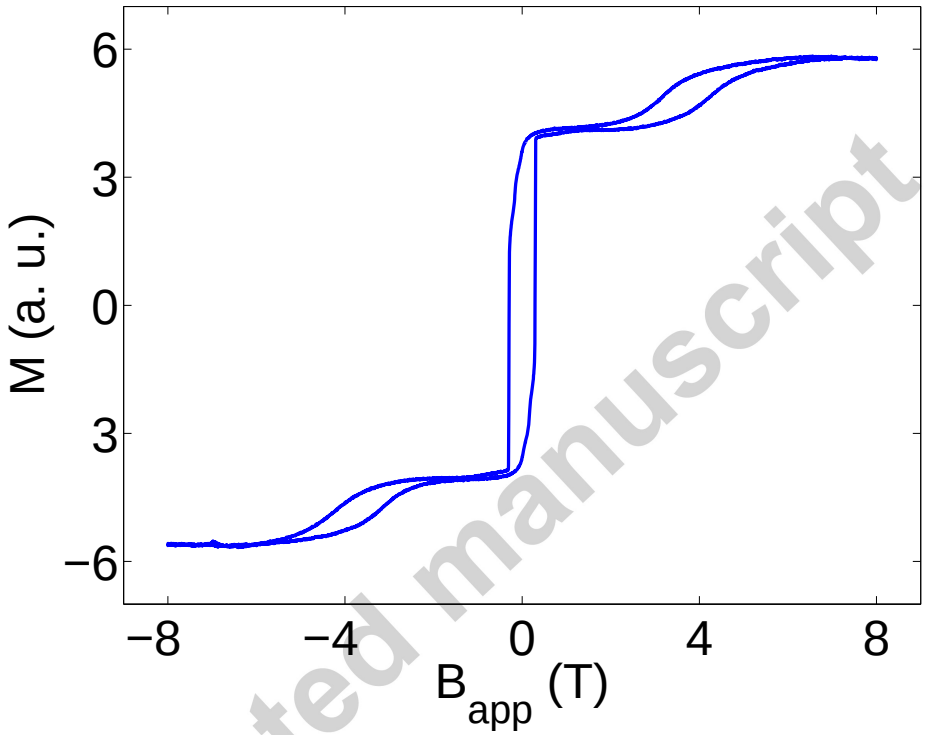

Figure 1: VSM hysteresis loop for the superlattice [$DyFe_2$ 40 Å/YFe_2 160 Å] × 20 with field along [$\bar{1}10$] at 250 K. According to micromagnetic simulation as shown in Fig. 2, the large field feature is similar to a spin-flop transition for the hard layers, while the small field behaviour involves coherent rotation and switching, characteristic of an exchange-spring magnet.

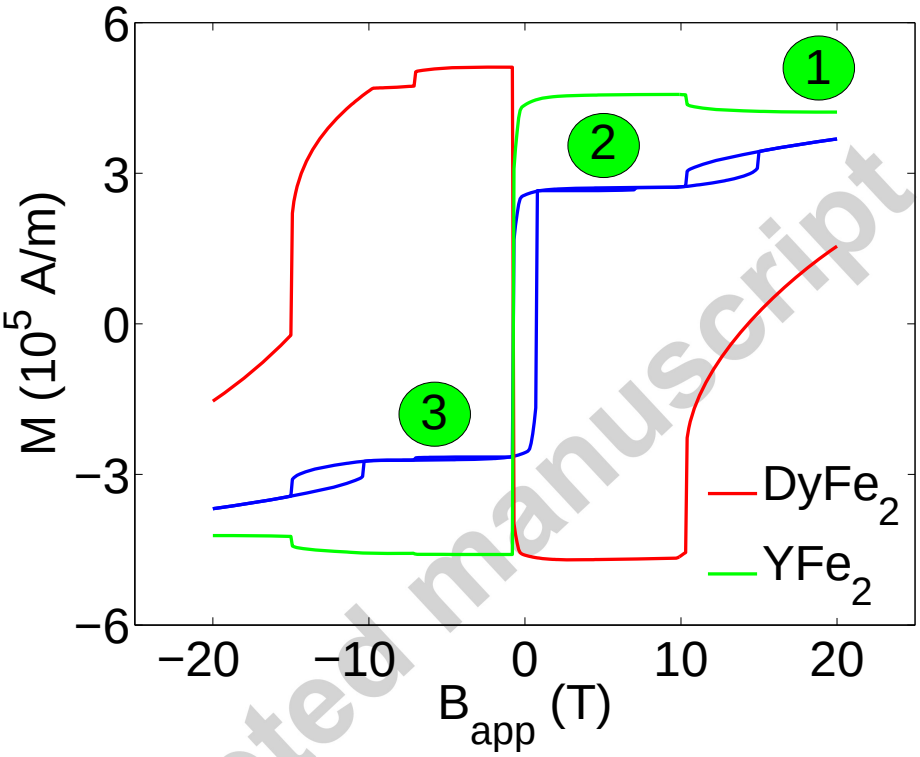

Figure 2: OOMMF simulated hysteresis loop for the superlattice [$DyFe_2$ 40Å/YFe_2 160 Å] × 20 with field along [$\bar{1}10$] at 380 K. The element specific demagnetization curves for $DyFe_2$ and YFe_2 are also shown. The circled numbers, showing the possible equilibrium positions for $DyFe_2$, correspond to those shown in Fig. 4.

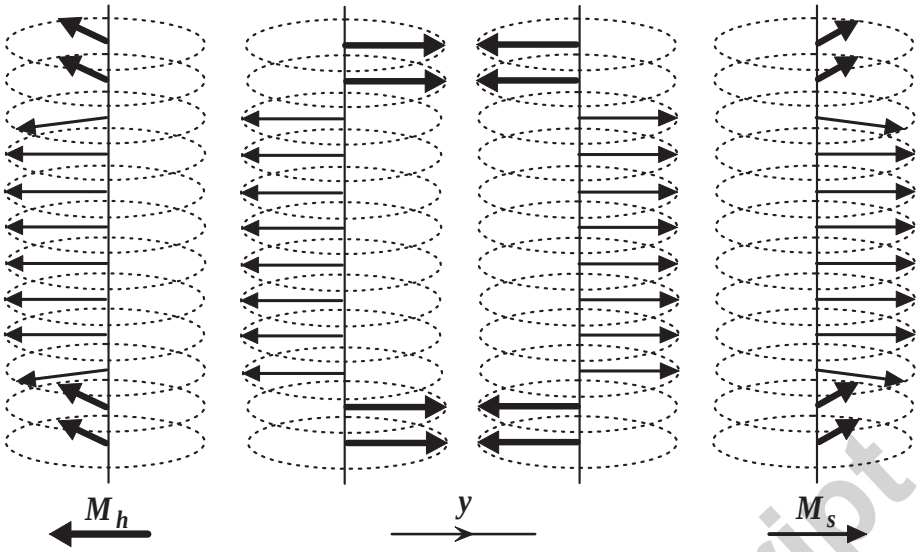

Figure 3: A schematic representation of the spin configuration for the demagnetization process of [$DyFe_2$ 40Å/YFe_2 160 Å] × 20 at 380 K with field along the [$\bar{1}10$] (y) direction. Thick and thin arrows denote the magnetic moments of $DyFe_2$ and YFe_2,respectively. The applied magnetic field decreases from 20 T to −20 T from right to left. Only the projection of the magnetic moments onto the film plane is shown.

netization parallel to [$\bar{1}10$], while that of the hard phase parallel to [001] (the first schematic illustration from right in Fig. 3, position circled 1 in Fig. 4) in the film plane. As a result, tight domain walls form at the interfaces. Upon decreasing the field to 10.3 T where the first switching happens, the soft phase remains unchanged, but the hard phase rotates further away from the applied field direction, forming an obtuse angle with respect to the soft magnetization. At 10.3 T, the hard phase switches to [$1\bar{1}0$] (the second illustration from right in Fig. 3, position circled 2 in Fig. 4). At the same time, the tightly wound domain walls are relaxed. So after the switching, the soft phase is mainly parallel to the field, with only small deviation at the interfaces, whereas the hard phase is antiparallel to the field, with a small component out of the film plane, towards [$0\bar{1}0$]. The transition at 10.3 T can be viewed as a spin-flop [9] switching mediated by exchange springs. This picture of the high field transition at 10.3 T, i.e. the presence of 90° domain walls, is consistent qualitatively with the neutron scattering analysis of the same system [10]. The moments at the interfaces are perfectly antiparallel to each other.

In the conventional sense, a spin-flop transition [9] refers to the transition from AFM arrangement of moments to noncollinear arrangement with a finite angle. The spin-flop transition discussed here is different. Although the angle between the central $DyFe_2$ moment and the in-plane easy direction is finite, the $DyFe_2$ and YFe_2 moments at the interfaces are still AFM and along the in-plane easy direction. Only when the two coupled layers are viewed as two macro-spins,

and the details of the arrangement of moments at the interfaces are ignored, can this transition be classified strictly as a spin-flop transition. For a reduced interface exchange, as considered in Ref. [10], the nomenclature of spin-flop will be more appropriate, too. If we focus our attention on the hard $DyFe_2$ phase, our situation is similar to the approach to saturation of a misaligned magnetic grain [24]. In the Stoner-wohlfarth model, when the applied magnetic field is misaligned with the uniaxial easy axis of a magnetic particle, the hysteresis loop is canted. Above the anisotropy field, the magnetization vector approaches to the direction of the applied positive field. On decreasing the applied field, the magnetization vector rotates to the easy direction, and finally switches to the almost antiparallel configuration when the applied field further decreases below the coercivity field. An analogy between the situation considered here and a misaligned particle can be drawn, if the $DyFe_2$ layers are to be viewed as a whole. The pinning provided by the soft phase can be taken as a negative exchange bias [25, 26], due to the AFM coupling at the interfaces. The applied positive field is thus modified by this exchange bias. For large positive field, the sum of the applied field and the exchange bias field is positive, and the hard layers rotate to the direction of the applied field, similar to the approach to saturation for a misaligned particle discussed above. When the field is reduced below a critical value, the exchange bias field dominates over the applied field, therefore the effective field felt by the hard layers will be negative enough and the magnetization will relax to one of the in-plane easy directions, antiparallel to the applied magnetic field. The resultant high-field minor hysteresis loop resembles that of a misaligned particle, as can be seen from Fig. 1.

A complete antiparallel configuration is achieved when the field is decreased to 9.8 T. This configuration is stable until the field is decreased to 0 T. Applying a negative field will move the moments out of plane, with the soft magnetization tilting towards [010] direction. The abrupt switching at -0.7 T corresponds to the simultaneous 180° rotation of the two phases so that after that switching, the configuration is completely antiparallel. The only change is that now it is the soft phase that is parallel with the applied negative field, along $[1\bar{1}0]$. The hard $DyFe_2$ is parallel to $[\bar{1}10]$ (the third illustration from right in Fig. 3, position circled 3 in Fig. 4). A larger negative field will pull the magnetization of the hard layer out of the film plane, towards [010] direction. If the out of plane angle is too large, further decreasing the applied (negative) field induces the switching observed at -15 T, after which the perpendicular configuration is restored, with the soft magnetization in plane and the hard magnetization parallel to [001] (the fourth illustration from right in Fig. 3, position circled 1 in Fig. 4) again. A schematic illustration of the whole demagnetization process is summarized in Fig. 3.

Clearly, as can be seen from the OOMMF simulation, the first (high field) transition corresponds to the spin-flop switching of $DyFe_2$, and the second (low field) corresponds to the simultaneous rotating of both $DyFe_2$ and YFe_2. This particular switching sequence can be explained by the energy surface of $DyFe_2$ at 380 K, as shown in Fig. 4. At such a high temperature, the effect of the magneto-elastic interaction is pronounced. Hence the easy axis has switched

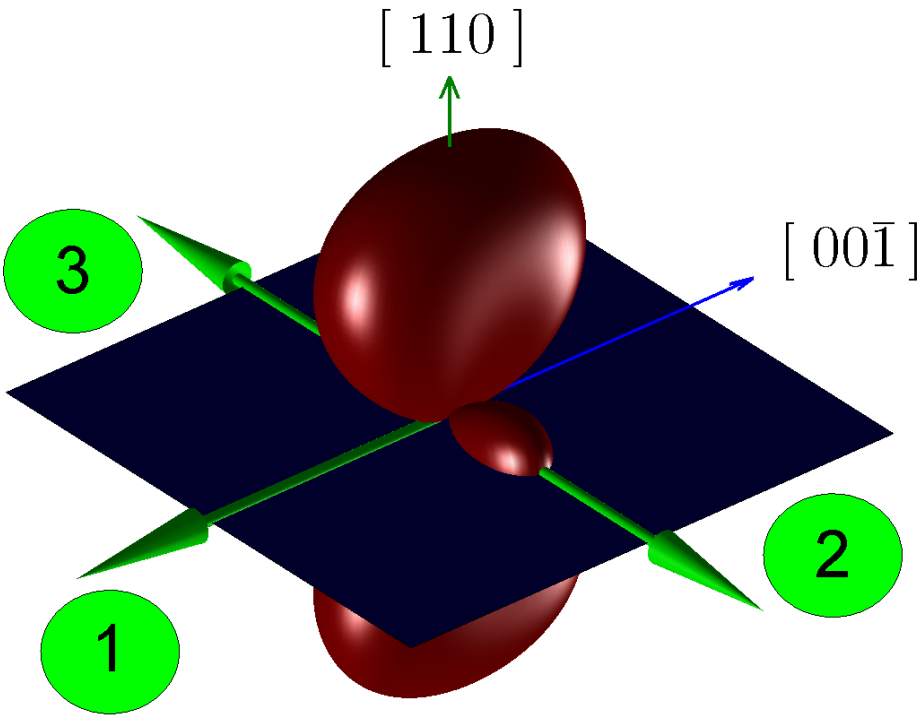

Figure 4: Energy surface for $DyFe_2$ at 380 K. The circled numbers signify the possible equilibrium directions for the magnetic moments to align with. The dark blue plane corresponds to the growth plane of the superlattice, i.e. the (110) plane. Positive applied field is along the [$\bar{1}$10] direction, which is parallel to the green arrow next to the circled number 3.

from the low temperature [001] to the high temperature one, 14° out of plane along [$\bar{1}$10] [18]. For field applied along [$\bar{1}$10] at 20 T, the soft phase is pulled almost parallel to the external field. Obviously, if a parallel configuration is to be achieved by rotating $DyFe_2$ to the direction of the external field, the exchange energy cost is too high, even for a field of 20 T. Due to the competition between the exchange, anisotropy and Zeeman energies, the observed perpendicular configuration results, in which the $DyFe_2$ moments are localized close to [001], a local anisotropy energy minimum as shown in Fig. 4.

4. Summary

In summary, exchange-spring driven spin-flop transition is observed in an YFe_2 dominant, antiferromagnetic $DyFe_2/YFe_2$ superlattice at high temperatures, for field along the [$\bar{1}$10] crystal direction. OOMMF simulation shows that the origin of the perpendicular configuration at high fields can be traced back to the strong magneto-elastic interaction, which is effective at high temperatures. The observed spin-flop transition is mediated by relaxation of exchange springs at the hard/soft interfaces. Standard exchange spring behavior is also observed for smaller fields. This gradual change in magnetization is given by the simultaneous rotation of both hard and soft moments towards the out-of-plane easy axis [010] for the crystalline anisotropy.

Acknowledegements

We wish to acknowledge the help on OOMMF simulation from Jürgen Zimmermann and Hans Fangohr. Financial support from EPSRC UK, under Grant No. GR/S95824, is gratefully acknowledged.

[1] E. F. Kneller and R. Hawig, IEEE Trans. Magn. **27**, 3588 (1991).

[2] R. Skomski and J. M. D. Coey, IEEE Trans. Magn. **29**, 2860 (1993); R. Skomski and J. M. D. Coey, Phys. Rev. B **48**, 15812 (1993); R. Skomski, J. Appl. Phys. **76**, 7059 (1994).

[3] D. Suess, T. Schrefl, S. Fahler, M. Kirschner, G. Hrkac, F. Dorfbauer, and J. Fidler, Appl. Phys. Lett. **87**, 012504 (2005); D. Suess, T. Schrefl, M. Kirschner, G. Hrkac, F. Dorfbauer, O. Ertl, and J. Fidler, IEEE Trans. Magn. **41**, 3166 (2005); D. Suess, J. Magn. Magn. Mater. **308**, 183 (2007).

[4] E. E. Fullerton, J. S. Jiang, M. Grimsditch, C. H. Sowers, and S. D. Bader, Phys. Rev. B **58**, 12193 (1998); M. Grimsditch, R. Camley, E. E. Fullerton, S. Jiang, S. D. Bader, and C. H. Sowers, J. Appl. Phys. **85**, 5901 (1999); E. E. Fullerton, J. S. Jiang, and S. D. Bader, J. Magn. Magn. Mater. **200**, 392 (1999).

[5] J-M. L. Beaujour, S. N. Gordeev, G. J. Bowden, P. A. J. de Groot, B. D. Rainford, R. C. C. Ward, and M. R. Wells, Appl. Phys. Lett. **78**, 964 (2001); S. N. Gordeev, J-M. L. Beaujour, G. J. Bowden, B. D. Rainford, P. A. J. de Groot, R. C. C. Ward, M. R. Wells, and A. G. M. Jansen, Phys. Rev. Lett. **87**, 186808 (2001).

[6] G. B. G. Stenning, G. J. Bowden, S. A. Gregory, J.-M. L. Beaujour, P. A. J. de Groot, G. van der Laan, L. R. Shelford, P. Bencok, P. Steadman, A. N. Dobrynin, and T. Hesjedal, Appl. Phys. Lett. **101**, 072412 (2012); G. B. G. Stenning, G. J. Bowden, S. A. Gregory, P. A. J. de Groot, G. van der Laan, L. R. Shelford, P. Bencok, P. Steadman, A. N. Dobrynin, and T. Hesjedal, Phys. Rev. B **86**, 174420 (2012).

[7] K. Dumesnil, C. Dufour, Ph. Mangin, F. Wilhelm, and A. Rogalev, J. Appl. Phys. **95**, 6843 (2004); K. Dumesnil, C. Dufour, P. Mangin, A. Rogalev, and F. Wilhelm, J. Phys.: Condens. Matter 17, L215 (2005).

[8] J. P. Zimmermann, G. Bordignon, R. P. Boardman, T. Fischbacher, H. Fangohr, K. N. Martin, G. J. Bowden, A. A. Zhukov, and P. A. J. de Groot, J. Appl. Phys. **99**, 08B904 (2006).

[9] D. L. Mills, Phys. Rev. Lett. **20**, 18 (1968); F. Keffer and H. Chow, *ibid.* **31**, 1061 (1973); S. G. E. te Velthuis, J. S. Jiang, S. D. Bader, and G. P. Felcher, *ibid.* **89**, 127203 (2002).

[10] M. R. Fitzsimmons, S. Park, K. Dumesnil, C. Dufour, R. Pynn, J. A. Borchers, J. J. Rhyne, and Ph. Mangin, Phys. Rev. B **73**, 134413 (2006).

[11] K. N. Martin, K. Wang, G. J. Bowden, A. A. Zhukov, P. A. J. de Groot, J. P. Zimmermann, H. Fangohr, and R. C. C. Ward, Appl. Phys. Lett. **89**, 132511 (2006); K. N. Martin, K. Wang, G. J. Bowden, P. A. J. de Groot, J. P. Zimmermann, H. Fangohr, and R. C. C. Ward, J. Appl. Phys. **101**, 09K511 (2007).

[12] G. B. G. Stenning, A. R. Buckingham, G. J. Bowden, R. C. C. Ward, G. van der Laan, L. R. Shelford, F. Maccherozzi, S. S. Dhesi, and P. A. J. de Groot, Phys. Rev. B **84**, 104428 (2011).

[13] M. J. Bentall, R. C. C. Ward, E. J. Grier, and M. R. Wells, J. Phys.: Condens. Matter **15**, 6493 (2003).

[14] U. Atzmony and M. P. Dariel, Phys. Rev. B **13**, 4006 (1976).

[15] K. N. Martin, P. A. J. de Groot, B. D. Rainford, K. Wang, G. J. Bowden, J. P. Zimmermann, and H. Fangohr, J. Phys.: Condens. Matter **18**, 459 (2006); G. J. Bowden, P. A. J. de Groot, B. D. Rainford, K. Wang, K. N. Martin, J. P. Zimmermann, and H. Fangohr, *ibid.* **18**, 5861 (2006).

[16] A. Mougin, C. Dufour, K. Dumesnil, N. Maloufi, Ph. Mangin, and G. Patrat, Phys. Rev. B **59**, 5950 (1999).

[17] V. Oderno, C. Dufour, K. Dumesnil, Ph. Bauer, Ph. Mangin, and G. Marchal, Phys. Rev. B **54**, R17375 (1996); A. Mougin, C. Dufour, K. Dumesnil, and Ph. Mangin, *ibid.* **62**, 9517 (2000).

[18] A. A. Zhukov, G. J. Bowden, J.-M. L. Beaujour, B. D. Rainford, P. A. J. de Groot, R. C. C. Ward, M. R. Wells, and H. Küpfer, J. Magn. Magn. Mater. **270**, 312 (2004).

[19] G. J. Bowden, A. A. Zhukov, J.-M. L. Beaujour, J. D. O'Neill, B. D. Rainford, P. A. J. de Groot, R. C. C. Ward, M. R. Wells, and H. Küpfer, J. Magn. Magn. Mater. **272-276**, E1591 (2004).

[20] J. P. Zimmermann, K. N. Martin, G. Bordignon, M. Franchin, R. C. C. Ward, G. J. Bowden, P. A. J. de Groot, and H. Fangohr, J. Magn. Magn. Mater. **321**, 2499 (2009).

[21] M. J. Donahue and D. G. Porter, *OOMMF User's Guide*, Version 1.0, National Institute of Standards and Technology, Gaithersburg, MD, 1999; Interagency Report NISTIR 6376.

[22] D. Wang, C. G. Morrison, A. R. Buckingham, G. J. Bowden, R. C. C. Ward, and P. A. J. de Groot, J. Magn. Magn. Mater. **321**, 586 (2009).

[23] W. F. Brown, Jr., *Micromagnetics* (Interscience, New York, 1963), pp. 143.

[24] J. Stöhr and H. C. Siegmann, *Magnetism: From Fundamentals to Nanoscale Dynamics*, Springer-Verlag Berlin Heidelberg, 2006.

[25] K. Dumesnil, C. Dufour, S. Fernandez, M. Oudich, A. Avisou, A Rogalev, and F. Wilhelm, J. Phys.: Condens. Matter 21, 236002 (2009).

[26] M. R. Fitzsimmons, C. Dufour, K. Dumesnil, J. Dou, and M. Pechan, Phys. Rev. B 79, 144425 (2009).